A NUMERICAL PROCEDURE FOR THE THREE-DIMENSIONAL THERMAL ANALYSIS OF SPACE STRUCTURES

D. Givoli O. Rand
Department of Aerospace Engineering
Technion — Israel Institute of Technology
Haifa 32000, Israel

Abstract

A new method is proposed for the numerical thermal analysis of three-dimensional large truss-type space structures exposed to solar radiation. Orthotropic truss members with a closed thin-walled cross section of arbitrary shape are considered. Three-dimensional thermal effects are taken into account in the analysis. In the proposed method, the governing equations are first put into a weak form. Then the Galerkin finite element method is applied with respect to the axial coordinate of each truss member. The circumferential variation of the temperature is treated by a symbolically-coded harmonic balance procedure. The interaction between the various truss members is controlled by an iterative scheme. The numerical examples include a comparison of the results obtained for a three-dimensional model and those obtained by standard one- and two-dimensional analyses.

Introduction

Thermal computational analysis has become an essential tool in the design process of large truss-type space structures. The thermal problems involved are usually highly nonlinear due to the presence of thermal radiation and nonlinear material behavior. In addition, the three-dimensional discretization of a large space structure would typically require a very large number of degrees of freedom if accurate results are desired. For an overview of the factors involved in this type of analysis see e.g. Refs. 1–3. Methods have been devised for the one-dimensional thermal analysis of space trusses,[4–6] and for the two-dimensional (cross-sectional) analysis of frame and truss structures.[7,8] The review paper by Pinson[9] should also be consulted.

The underlying assumption in a *one-dimensional* thermal analysis is that the temperature variation within the cross section of any of the rods comprising the structure may be neglected in comparison with the variation along the axial direction of the rod. This assumption is justified for space structures composed of sufficiently slender rods and made of thermally high-conductive materials such as metals. If one proceeds to compute the elastic deformation and stresses generated by the temperature field thus derived, the structural response in terms of tension, compression and buckling of various truss members can be obtained.

A different approach is based on a *two-dimensional* analysis, and in a sense is complementary to the previous analysis. This approach starts from the assumption that the temperature variation along the axial direction of each rod is negligible with respect to the variation through the cross section. This assumption has been shown to be appropriate for structures with slender thin-walled members made of laminated composite materials such as graphite/epoxy.[10] This type of response in a fiber/matrix material originates from the low thermal conductivity of the material in the axial direction. The temperature variation through the cross sections of the structural members produces in turn elastic bending. The corresponding displacements and stresses can be obtained by performing a structural analysis on the basis of the results from the thermal analysis.

The present paper proposes a numerical procedure for the *three-dimensional* thermal analysis of truss-type space structures. This means that both the axial and cross-sectional variations of the temperature are taken into account. The proposed procedure makes an effective tool for the analysis of both metallic and composite space structures with either long or short members. It can also be used as a first step in a detailed three-dimensional thermoelastic analysis.

A straight-forward use of a standard numerical method, such as the finite element method, for the solution of the governing equations in the three-dimensional domain defined by the structure, typically requires a very large computational effort, due to the tremendous number of degrees of freedom involved (See e.g. Chin et al.[11]). To avoid this aspect of the analysis, a special procedure is adopted in this paper. First, the governing equations are put into a weak form. Then a Galerkin finite element discretization is applied, but only with respect to the *axial coordinate* of each truss member *separately*. This results in a non-standard finite element formulation. The *circumferential variation* of the temperature is decomposed spectrally, and the Fourier coefficients of this decomposition are found by a symbolically-coded harmonic balance procedure developed in Rand and Givoli.[12] Finally, the interaction between the various truss members is controlled by an iterative scheme. [13]

The numerical examples presented here demonstrate the performance of the proposed method, and include a comparison of the results obtained by the three-dimensional analysis to those obtained by the corresponding one- and two-dimensional models. This comparison shows that in some situations one- and two-dimensional analyses do not provide sufficient or accurate information on the temperature distribution, and a three-dimensional analysis is thus required.

Finite Element Formulation

Consider a composite truss-type structure where each truss member has a uniform thin-walled closed cross section of an arbitrary shape. Fig. 1 shows a typical member in the structure. The axial coordinate is denoted ξ, and the circumferential coordinate along the midline of the thin cross section is denoted s. The latter coordinate starts from an arbitrary point on the midline and measures arclength along this line. The maximal value of s, namely the cross sectional perimeter, is denoted p. The member's length is L and the thickness of the cross section is t. The exterior surface of the rod is exposed to solar radiation.

Some simplifying assumptions are made in the present model. The edges $\xi = 0$ and $\xi = L$ are assumed to converge geometrically to fit into the joints which connect the rod to other structural members. In these edges the cross section is characterized by a single temperature, assumed to be identical for all the rods connected to the same joint. In other words, the joints are considered perfect conductors and lacking any heat capacity. In addition, it is assumed that two usually weak effects can be neglected, namely heat exchange through radiation between different truss members, and the thermodynamic influence of the elastic strain rate on the temperature field.

The equation of steady-state heat conduction and radiation which holds in the three-dimensional domain defined by the rod is

$$\nabla \cdot (\boldsymbol{\kappa} \nabla u) - C_R u^4 + q = 0 \ . \qquad (1)$$

Here $u(\xi, s)$ is the temperature, $\boldsymbol{\kappa} = [\kappa_{ij}]$ is the thermal conductivity tensor for the anisotropic material under consideration, C_R is the radiation coefficient, and q is the given solar incident flux. The coefficient C_R is given by

$$C_R = \frac{\sigma \epsilon}{t} \qquad (2)$$

where σ is the universal Stefan-Boltzmann constant, and ϵ is the surface emissivity of the member. The incident flux q is calculated by

$$q(s) = \frac{\alpha \beta_o \beta_s(s)}{t} \, q_{\text{sun}} \ . \qquad (3)$$

Here q_{sun} is the absolute value of the solar radiation vector, α is the surface absorptivity, β_o is the "view factor" associated with the orientation of the rod with respect to the solar radiation vector, and $\beta_s(s)$ is the "view factor" depending on the direction of the normal $\boldsymbol{n}$ to the outer surface of the cross section at each point on the surface. (See Fig. 1.) Both "view factors" can have values between zero and one.

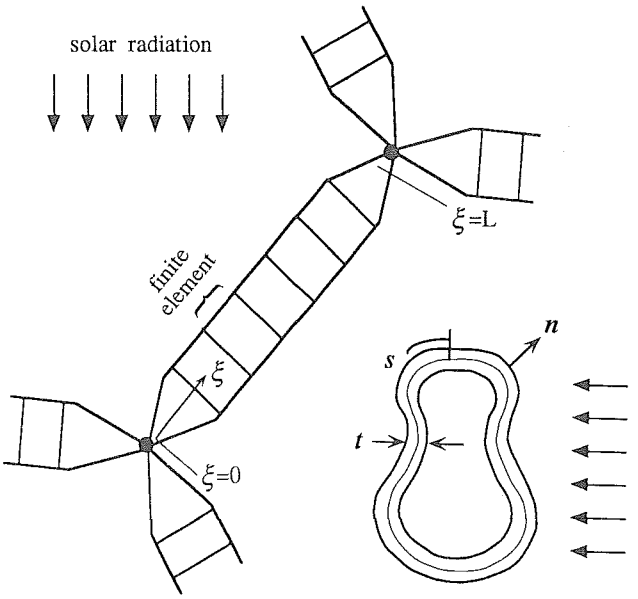

Figure 1. A typical member in the structure, exposed to solar radiation.

Equation (1) is supplemented by two boundary conditions at the edges $\xi = 0$ and $\xi = L$ and also by the requirement that the temperature $u(\xi, s)$ is a periodic function in s with period p. The two boundary conditions at the edges are Dirichlet conditions, namely

$$u(0, s) = T_1 \quad ; \quad u(L, s) = T_2 \qquad (4)$$

where T_1 and T_2 are regarded, for the time being, as *given* temperatures.

For simplicity, it is further assumed that the conductivity tensor $\boldsymbol{\kappa}$ in (1) has its principal directions along the ξ and s axes. In other words, the composite fiber-matrix configuration of the rod is such that each rod is associated with two effective conductivities: the axial conductivity κ_ξ and the circumferential conductivity κ_s. Also, it should be noted that for thin-walled members the exact shape of the cross section is irrelevant as far as heat conduction is concerned; the detailed cross sectional geometry is important only for the determination of the radiation view factor β_s in (3). In this light, the first term in eq. (1) becomes

$$\nabla \cdot (\boldsymbol{\kappa} \nabla u) \equiv \frac{\partial}{\partial \xi} \left(\kappa_\xi \frac{\partial u}{\partial \xi} \right) + \frac{\partial}{\partial s} \left(\kappa_s \frac{\partial u}{\partial s} \right) \ . \qquad (5)$$

Now the Galerkin finite element is applied to eqs. (1) and (4) *with respect to ξ only*. Thus, each rod is divided into one-dimensional finite elements in the ξ direction, whereas variation with respect to the variable s remains continuous. This results in the following system of ordinary differential

equations in the variable s:

$$\boldsymbol{M}\,\boldsymbol{d}_{ss}(s) + \boldsymbol{K}\,\boldsymbol{d}(s) + \boldsymbol{R}\,(\boldsymbol{d}(s)) = \boldsymbol{F}(s) \qquad (6)$$

where

$$\begin{aligned} \boldsymbol{M} &= \mathcal{A}_{e=1}^{N_{el}} \boldsymbol{m}^e \quad ; \quad \boldsymbol{K} = \mathcal{A}_{e=1}^{N_{el}} \boldsymbol{k}^e \\ \boldsymbol{R} &= \mathcal{A}_{e=1}^{N_{el}} \boldsymbol{r}^e \quad ; \quad \boldsymbol{F} = \mathcal{A}_{e=1}^{N_{el}} \boldsymbol{f}^e \ . \end{aligned} \qquad (7)$$

Here N_{el} is the total number of elements in the rod in the ξ direction, $\mathcal{A}_{e=1}^{N_{el}}$ is the assembly operator, and $\boldsymbol{m}^e$, $\boldsymbol{k}^e$, $\boldsymbol{r}^e$ and $\boldsymbol{f}^e$ are the element matrices and vectors corresponding to the global matrices and vectors $\boldsymbol{M}$, $\boldsymbol{K}$, $\boldsymbol{R}$ and $\boldsymbol{F}$. The subscript ss in (6) stands for the second derivative with respect to s. In (6), $\boldsymbol{d}$ is the global solution vector containing the nodal temperatures, and $\boldsymbol{R}$ is the radiation vector which depends nonlinearly on $\boldsymbol{d}$ (see (10) below). The expressions for the element matrices and vectors are:

$$m_{ab}^e = -\int_{\Omega^e} N_a\,\kappa_s\,N_b\,d\xi \qquad (8)$$

$$k_{ab}^e = \int_{\Omega^e} N_a'\,\kappa_\xi\,N_b'\,d\xi \qquad (9)$$

$$r_a^e = \int_{\Omega^e} N_a\,C_R \left(\sum_{b=1}^{N_{en}} T_b(t) N_b(s)\right)^4 d\xi \qquad (10)$$

$$f_a^e = \int_{\Omega^e} N_a q\,d\xi - \sum_{b=1}^{N_{en}} T_b^e k_{ab} \qquad (11)$$

Here Ω^e is the element domain, N_a is the element shape function associated with node a, N_{en} is the number of element nodes, and

$$T_b^e = \begin{cases} T_1 & \text{if } e = 1 \text{ and } b = 1 \\ T_2 & \text{if } e = N_{el} \text{ and } b = N_{en} \\ 0 & \text{otherwise} \end{cases} \ . \qquad (12)$$

The prime in (9) indicates differentiation with respect to ξ.

The finite element matrix formulation (6)–(12) is clearly non-standard is some aspects, although it has a remarkable resemblance to the standard semi-discrete formulation in the *one-dimensional time-dependent* case, where s is analogous to *time* (see e.g. Hughes.[14]) Explicit expressions for (8)–(11) for a specific choice of shape functions can easily be obtained. For example, in the case where $N_{en} = 2$ and N_a $(a = 1, 2)$ are the linear shape functions, and assuming that κ_s has the constant value κ_s^e in element e, eq. (8) gives

$$\boldsymbol{m}^e = -\frac{\kappa_s^e h^e}{6} \begin{bmatrix} 2 & 1 \\ 1 & 2 \end{bmatrix} \qquad (13)$$

where h^e is the element length. Fuller details on the finite element formulation can be found in Rand and Givoli.[13]

The Harmonic-Balance Procedure

The solution of the system of ordinary differential equations (6) has to be considered next. The method of solution of this system is based on the spectral method devised by Rand and Givoli[12] in the time-periodic one-dimensional context. In this method, each s-dependent function in (6) is decomposed, using the discrete Fourier transform, into a finite number of harmonics, N, and the Fourier coefficients are found using a nonlinear harmonic balance analysis.

To be more specific, consider any vector $\boldsymbol{g}(s)$ appearing in eq. (6). This vector is approximately represented by the finite Fourier expansion,

$$\boldsymbol{g}(s) \simeq \boldsymbol{g}_0 + \sum_{n=1}^{N} (\boldsymbol{g}_{cn} \cos n\phi + \boldsymbol{g}_{sn} \sin n\phi) \ . \qquad (14)$$

Here $\boldsymbol{g}_0$, $\boldsymbol{g}_{cn}$ and $\boldsymbol{g}_{sn}$ $(n = 1, ..., N)$ are real constant vectors, and ϕ is the circumferential angle defined by $\phi = 2\pi s/p$. All the variables in eq. (6), namely all the entries of the vectors $\boldsymbol{d}$, $\boldsymbol{R}$ and $\boldsymbol{F}$, are expanded via (14). The Fourier coefficients $\boldsymbol{F}_0$, $\boldsymbol{F}_{cn}$ and $\boldsymbol{F}_{sn}$ associated with the thermal load vector $\boldsymbol{F}$ are found using a Fast Fourier Transform (FFT) scheme. All the calculations involved have been performed symbolically by the computer code itself. We have used the symbolic manipulation program described in Ref. 12 which is particularly suitable for harmonic-type calculations.

After the Fourier expansions of $\boldsymbol{d}$, $\boldsymbol{R}$ and $\boldsymbol{F}$ are substituted in (6), one obtains a nonlinear coupled system of algebraic equations for the unknown coefficient vectors $\boldsymbol{d}_0$, $\boldsymbol{d}_{cn}$ and $\boldsymbol{d}_{sn}$. Again, the formation of all these algebraic equations is performed symbolically by the code[13]. The algebraic system of equations thus obtained is solved via a modified Newton-Raphson iterative procedure.

Joint Temperature Updating Scheme

In the solution procedure outlined above for the temperature variation in the ξ and s directions it was assumed that all the joint temperatures were *given*. These joint temperatures were used in the boundary conditions (4) prescribed at the edges of each rod and appeared in the finite element formulation in (11), (12). However, the joint temperature are in fact unknown, and therefore an iterative scheme is needed to update them. The scheme starts from an "initial guess" for all joint temperatures. Based on these data, the finite-element spectral analysis is performed for each rod separately, and the temperature field in the entire structure is found. Next all the joint temperatures are updated, according to the guidelines given below, and the finite-element spectral procedure is repeated. This yields a better solution, on the basis of which the joint temperatures are updated again, and so on. This process stops when convergence is achieved, namely when the differences between joint temperatures obtained in two successive iterations are sufficiently small.

The scheme adopted here for updating the joint temperatures is as follows. Consider a certain joint which connects together J rods. It is clear that the net amount of heat flux entering the joint from all J rods must be zero. This can be stated by

$$\sum_{j=1}^{J} \int_{A_j} \kappa_\xi \frac{\partial u^*}{\partial \xi} \, dA_j = 0 \ , \qquad (15)$$

where A_j is the cross-sectional area of rod j, and u^* is the approximate solution near the joint obtained by the finite-element spectral method. Now for the thin closed cross section considered here we have $dA_j = (t_j p_j / 2\pi) d\phi$, where t_j and p_j are respectively the thickness and perimeter of rod j. Also, we replace $\partial u^* / \partial \xi$ by the finite difference approximation $\left(u^*|_{\xi=\Delta_j} - U\right) / \Delta_j$. Here Δ_j is the length of the first finite element belonging to rod j and starting from the joint, and U is the value of the temperature at the joint, which is common to all the rods $j = 1, ..., J$. For simplicity we assume that κ_ξ in rod j has the constant value $\kappa_{\xi j}$ in the first element near the joint.

Now recall that $u^*(\xi, \phi)$ is composed of N ϕ-harmonics as in eq. (14), i.e.:

$$u^* = u_0^* + \sum_{n=1}^{N} (u_{cn}^* \cos n\phi + u_{sn}^* \sin n\phi) \ . \qquad (16)$$

Only the zeroth-order harmonic u_0^* will contribute to the integral in (15), the average of all higher harmonics being zero. Thus (15) gives

$$\sum_{j=1}^{J} \frac{t_j p_j \kappa_{\xi j}}{\Delta_j} \left(u_0^*|_{\xi=\Delta_j} - U\right) = 0 \ . \qquad (17)$$

Eq. (17) can be solved for the joint temperature U, i.e.

$$U = \frac{\sum_{j=1}^{J} (t_j p_j \kappa_{\xi j} / \Delta_j) \, u_0^*|_{\xi=\Delta_j}}{\sum_{j=1}^{J} t_j p_j \kappa_{\xi j} / \Delta_j} \ . \qquad (18)$$

This formula holds for every joint separately. Thus, eq. (18) is used for updating all the joint temperatures on the basis of the results obtained from the preceding finite-element spectral analysis.

Various numerical experiments show that the iterative procedure outlined above which incorporates the updating formula (18) converges rapidly if the initial guess for the joint temperatures is reasonably close to the exact solution there. However, when the initial guess is significantly different from the exact solution the process may diverge. This divergence can be prevented by limiting the allowed change per iteration for each joint temperature.[13]

Numerical Examples

We first consider the graphite-epoxy parabolic dish structure shown in Fig. 2. The thermal and geometrical data are: $\alpha = 0.28$, $\beta_0 = 1$, $t = 0.015$m, $q_{\text{sun}} = 1300\text{W/m}^2$, $\kappa_\xi = \kappa_s = 10.1\text{W/m °K}$, and $C_R = 9.1 \cdot 10^{-7}\text{W/m}^3\ °\text{K}^4$. The radii of the inner and outer rings are 5m and 20m, respectively, and the depth between these rings is 6m. The global cartesian coordinate system $x-y-z$ is introduced as shown in Fig. 2. All the truss members have a thin circular cross-section of radius 0.1m. Each member in the structure is divided into seven finite elements with linear shape functions. These elements are not equally spaced, but rather graded using a cosine distribution in which the density of the elements is larger near the two edges than in the middle of the rod. In Fig. 2 the rods numbered 1, 16, 22 and 61 are indicated for future reference. We use 12 harmonics in the Fourier expansions of all the variables.

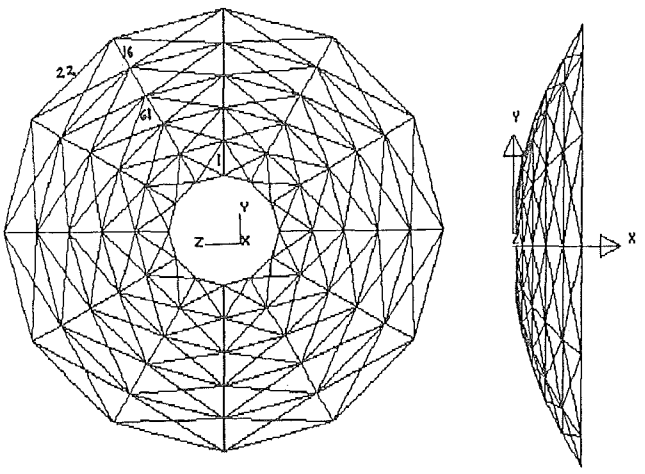

Figure 2. The parabolic antenna dish model.

The solar radiation points in the $-z$ direction. The dish is assumed to have a constant orientation with respect to the radiation vector, or else its orientation is assumed to change in time sufficiently slowly so that the response can be considered quasi-steady. We use the procedure proposed previously to obtain the three dimensional distribution of temperatures in the structure. Based on the results of this analysis, Fig. 3 shows the average temperature in the cross section (u_0^* in eq. (16)) as a function of the axial coordinate ξ for rods 1, 16, 22 and 61. Fig. 4 shows the temperature distribution around the cross section for the middle sections ($\xi = L/2$) of rods 1, 16, 22 and 61. The results demonstrate that the position of the rod in the structure and its orientation have a significant influence on the temperature distribution both in the axial direction and in the circumferential direction.

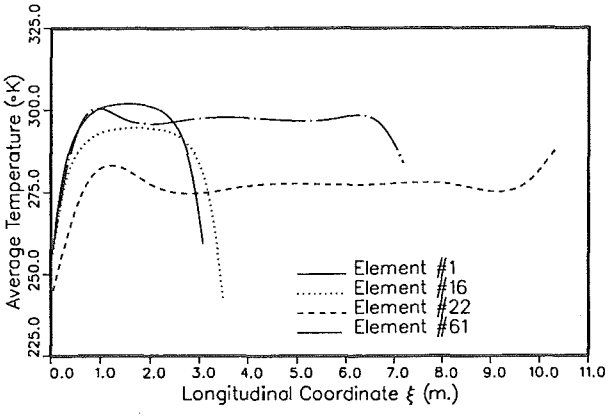

Figure 3. Three-dimensional analysis: average cross-sectional temperatures along the axes of rods 1, 16, 22 and 61.

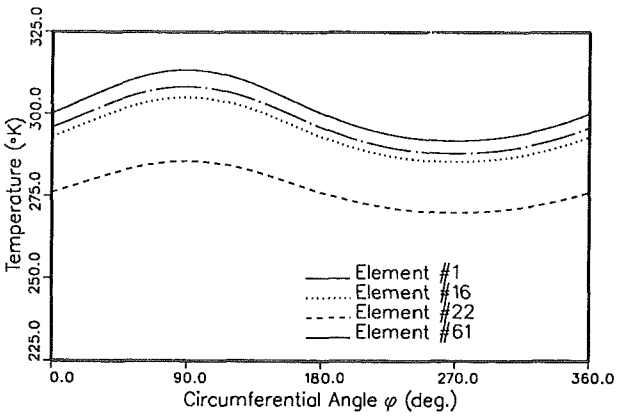

Figure 4. Three-dimensional analysis: mid-rod temperature along the cross-sectional perimeter of rods 1, 16, 22 and 61.

Next we compare the results obtained above to those which may be obtained by simpler one- and two-dimensional analyses. The *one-dimensional* approach ignores temperature distribution through the cross section. The results for the temperature as a function of the axial coordinate ξ for rods 1, 16, 22 and 61 obtained from a one-dimensional analysis turn out to coincide with those for the three-dimensional *average* temperature shown in Fig. 3. This is in fact expected since the one-dimensional model is supposed to describe the average behavior in the cross section of the three-dimensional model. However, the one-dimensional approach does not provide any information on the cross-sectional temperature variation.

Finally we consider the *two-dimensional* approach, which assumes uniformity of the temperature field in the rod axial direction. In Fig. 5 the temperature around the cross section (at any location) of rod 61 obtained by the two-dimensional analysis, is compared to the temperature distribution obtained by the three-dimensional analysis around the cross sections at eight locations of rod 61. These eight locations on the axis of the rod are the locations of the finite element nodal points. It is apparent from Fig. 5 that the two-dimensional distribution coincides with the

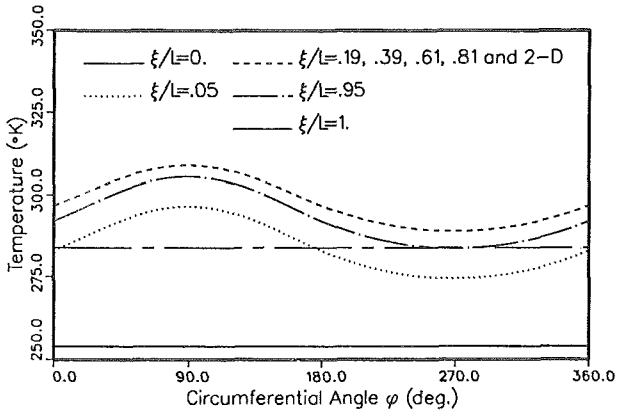

Figure 5. Comparison between the temperature distribution along the perimeter of rod 61 as obtained by the two-dimensional analysis and that obtained by the three-dimensional analysis at eight axial locations.

three-dimensional distribution at nodes 3–6 (in the central region of the rod), but that at the other four locations the results of the two analyses differ significantly. Moreover, in the two-dimensional approach information regarding the variation of temperatures or thermal stresses in the axial direction is unavailable.

As a second example, we apply the numerical method to the multi-bay structure illustrated in Fig. 6. The global Cartesian system of coordinates (x, y, z) is also shown in the figure. All the members have a thin-walled circular cross section of radius $R = 0.0045$m and thickness $t = 0.001$m. The global dimensions of the structure are 2m×2m×5m. The thermal material properties are: $\alpha = 0.018$, $\kappa_\xi = \kappa_s = 10.1$W/m °K, $\sigma\epsilon = 9.1 \cdot 10^{-10}$W/m^2°K^4.

The structure is exposed to solar radiation of magnitude $q_{\text{sun}} = 1300$ W/m^2, directed in the $-x$ direction. The structure material is opaque and self-shadowing effects are taken into account. Thus, half of the entire structure and also half of the outer perimeter of every cross section are hidden from the incident heat flux. As before, each member was divided in its axial direction into 7 finite elements, using a cosine-type distribution. In the harmonic-balance procedure used in the circumferential direction, the first 12 harmonics were taken into account.

As already mentioned half of the structure is in the shadow. However, one should note that the 10 members lying in the $x = 0$ plane (arranged in two columns of five members each) are exactly on the boundary line between the exposed and hidden regions of the structure. Whether they are themselves exposed or hidden is therefore extremely sensitive to small geometrical perturbations. Here we consider two cases: the symmetric case in which both columns of beams are exposed to the sun, and the asymmetric case in which only the left one (see Fig. 6) is exposed whereas the right column is hidden.

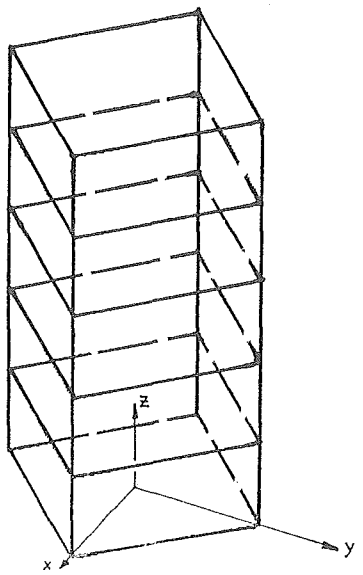

Figure 6. A multi-bay frame structure, exposed to solar radiation coming from the x direction.

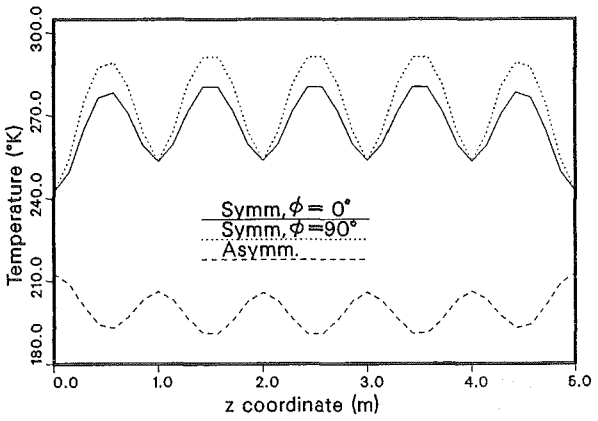

Figure 7. The temperature distribution along the right column of beams at $\phi = 0°$ and $\phi = 90°$, in the symmetric and asymmetric cases.

Fig. 7 shows the temperature distribution along the right column of beams at two cross-sectional circumferential positions, namely at $\phi = 0°$ and $\phi = 90°$. Results in both the symmetric and asymmetric cases are shown. In the latter case the right column is entirely in the shade and hence the temperature is circumferentially uniform. In the symmetric case, the temperatures at the two circumferential locations differ by more than 10°K. The average temperature in the asymmetric case is smaller by about 70°K.

Concluding Remarks

In this paper we have proposed a special numerical procedure for the solution of thermal problems of truss-type space structures, which takes into account three-dimensional effects. The proposed method avoids the need for a large number of degrees of freedom which is typical when using the standard finite element and finite difference methods in three dimensions. It was shown that in some situations one- and two-dimensional analyses do not provide sufficient or accurate information on the temperature distribution, and a three-dimensional analysis is required. Another important advantage of the proposed method is that it can serve as a first step in producing detailed three-dimensional thermoelastic information. See Ref. 13 for fuller details.

An important addition to this work would be the extension to the *dynamic* case, and in particular to the case of periodic motions. It seems that an application of the harmonic balance procedure with respect to both the circumferential coordinate (s) and time (t) may be beneficial. We hope to report on progress in this direction in the future.

Acknowledgments

This work was supported in part by the Adler Fund for Space Research managed by the Israel Academy of Sciences. We also wish to acknowledge the assistance of Mrs. Cecilia Zolotnizki in programming.

References

1. P. Santini and A. Paolozzi, "Heat Conduction in a Large Space Structure," *Acta Astro.*, 19, pp. 162–170, 1989.

2. W.A. Nash and T.J. Lardner, "Parametric Investigation of Factors Influencing the Mechanical Behavior of Large Space Structures," *AFOSR report* no. TR-86-0858, 1985.

3. S.C. Peskett and D.T. Gethin, "Thermal Analysis of Spacecraft," *Numerical Methods in Thermal Problems*, eds. R.W. Lewis and K. Morgan, Vol. VI, part 1, Pineridge Press, pp. 713–729, 1989.

4. J. Mahaney and E.A. Thornton, "Self-Shadowing Effects on the Thermal-Structural Response of Orbiting Trusses," *J. Spacecraft and Rockets*, 24, pp. 342–348, 1987.

5. W.L. Ko, "Solution Accuracies of Finite Element Reentry Heat Transfer and Thermal Stress Analyses of Space Shuttle Orbiter," *Int. J. Num. Meth. Engrg.*, 25, pp. 517-543, 1988.

6. O. Rand and D. Givoli, "An Integrated Thermoelastic Analysis for Periodically Loaded Space Structures," in *proc. of 17th Congress of ICAS*, Stockholm, Sweden, pp. 1529–1533, 1990.

7. J. Mahaney, E.A. Thornton and P. Dechaumphai, "Integrated Thermal-Structural Analysis of Large Space Structures," in *Computational Aspects of Heat Transfer in Structures Symposium*, NASA Langley Research Center, Hampton, VA, NASA CP-2216, pp. 179–198, 1981.

8. J.D. Lutz, D.H. Allen and W.E. Haisler, "Finite-Element Model for the Thermoelastic Analysis of Large Composite Space Structures," *J. Spacecraft and Rockets*, 24, pp. 430–436, 1987.

9. L.D. Pinson, "Recent Advances in Structural Dynamics of Large Space Structures," *Acta Astro.*, 19, pp. 162–170, 1989.

10. E.W. Brogren, D.L. Barclay and J.W. Straayer, "Simplified Thermal Estimation Techniques for Large Space Structures," *NASA Rep.* CR-145253, 1977.

11. J.H. Chin, D.R. Frank and J.M. Winget, "Engineering Finite Element Analysis of Large Three-Dimensional Heat Transfer Problems," in *Numerical Methods in Thermal Problems*, R.W. Lewis and K. Morgan, eds., Pineridge Press, 1985, pp. 341–352.

12. O. Rand and D. Givoli, "A Finite Element Spectral Method With Application to the Thermoelastic Analysis of Space Structures," *Int. J. Num. Meth. Engrg.*, 30, pp. 291–306, 1990.

13. O. Rand and D. Givoli, "Thermal Analysis of Space Trusses Including Three-Dimensional Effects," *Int. J. Num. Meth. Heat Fluid Flow*, to appear.

14. T.J.R. Hughes, *The Finite Element Method*, Prentice Hall, Englewood Cliffs, New Jersey, 1987.